

# Barred galaxy formation in the EAGLE cosmological simulation



Mario G. Abadi

Astronomical Observatory, National University of Córdoba (UNC)  
Institute for Theoretical and Experimental Astronomy (IATE)  
CONICET-UNC Argentina



26-30 September, 2016

MultiDark Galaxies Workshop La Plata, Argentina

# Collaborators

Aim:

Search some clues about bar formation in cosmological numerical simulations

Barred galaxies in the EAGLE cosmological hydrodynamical simulation

Submitted MNRAS, astro-ph 160905909

**David G. Algorry (Córdoba)**, Julio F. Navarro (Victoria), Laura V. Sales (Riverside)  
Richard G. Bower (Durham), Robert A. Crain (Liverpool), Claudio Dalla Vecchia  
(Tenerife), Carlos S. Frenk (Durham), Matthieu Schaller (Durham), Joop Schaye  
(Leiden) and Tom Theuns (Durham).

# Hubble Morphological Classification

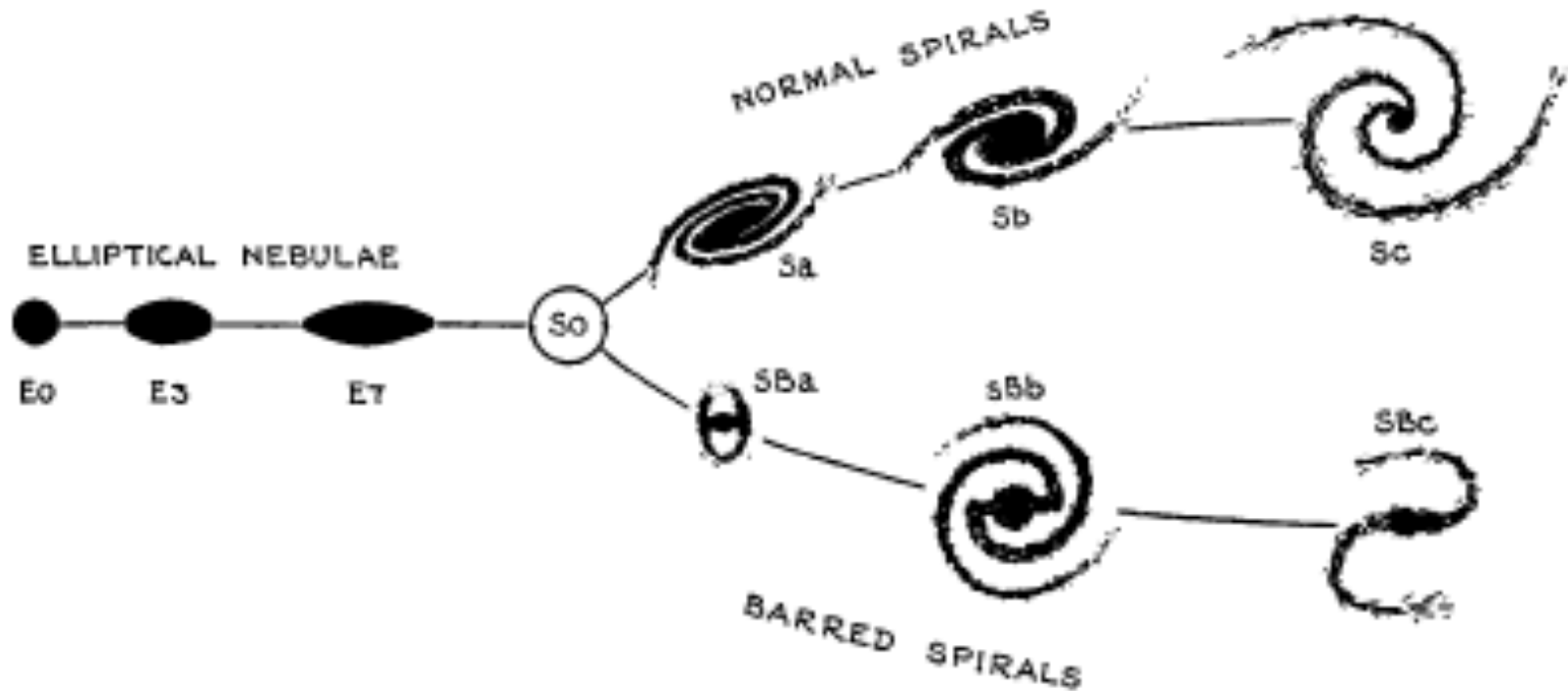
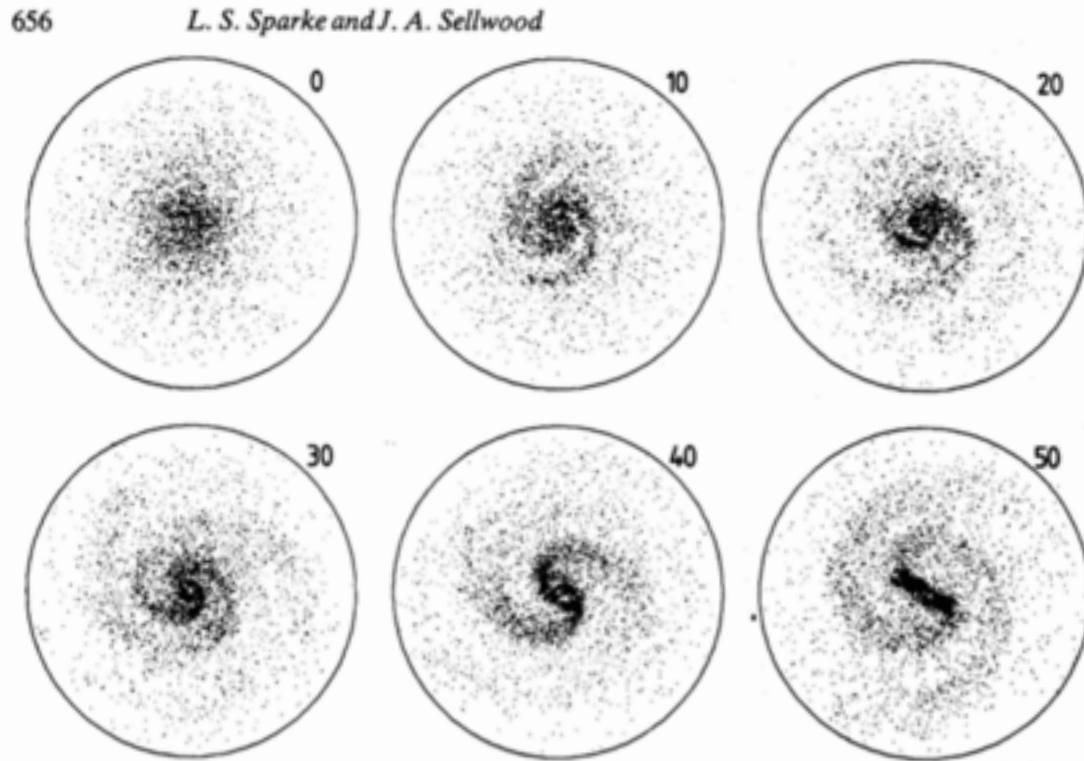


FIG. 1. *The Sequence of Nebular Types.*

The diagram is a schematic representation of the sequences of classification. A few nebulae of mixed types are found between the two sequences of spirals. The transition stage, S0, is more or less hypothetical. The transition between E7 and SB<sub>a</sub> is smooth and continuous. Between E7 and S<sub>a</sub>, no nebulae are definitely recognized.

# Isolated Disk Galaxy Models



2 dimensional disk

Self-gravitating particles

Rotation with low  
velocity dispersion

Numerical and analytical calculations during the past decade have established that cold self-gravitating disks are unstable to the formation of bars (Hohl and Hockney, 1969; Miller et al., 1970; Kalnajs, 1972; James and Sellwood, 1978). Combes & Sanders 1981

# Isolated Disk Galaxy Models

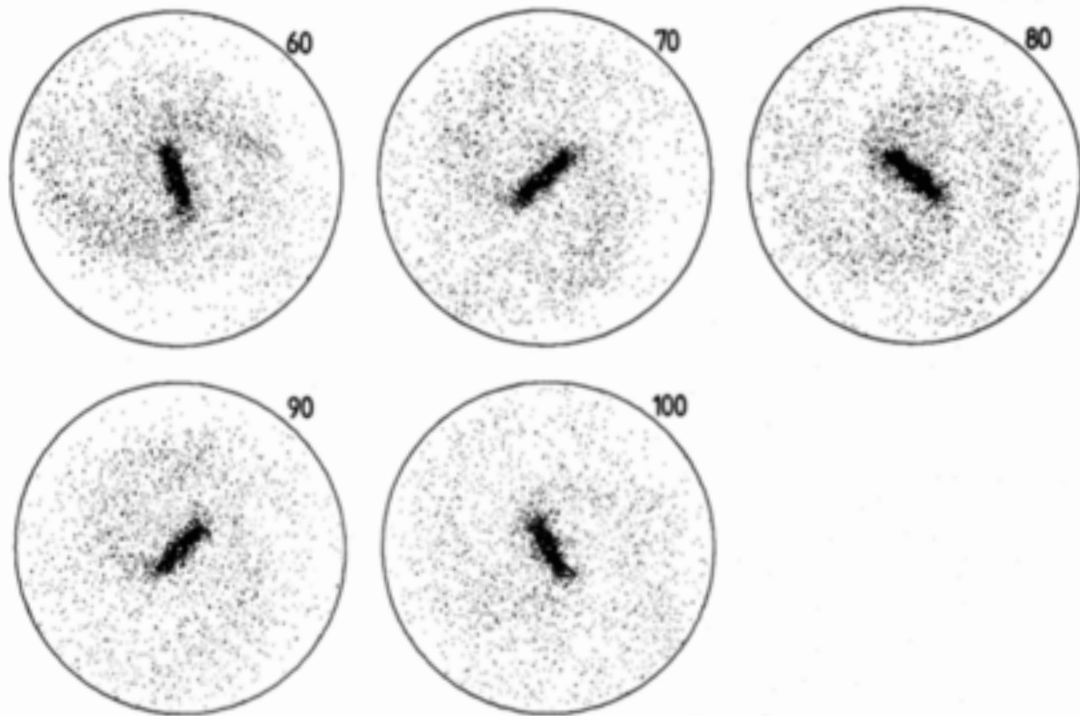


Figure 1. Development of the bar. The times are in natural units and the outer circle marks the boundary of the grid at a radius of 4.57. Only one particle in 10 is included in each frame and the bulge component is not shown.

2 dimensional disk

Self-gravitating particles

Rotation with low  
velocity dispersion

Numerical and analytical calculations during the past decade have established that cold self-gravitating disks are unstable to the formation of bars (Hohl and Hockney, 1969; Miller et al., 1970; Kalnajs, 1972; James and Sellwood, 1978). Combes & Sanders 1981

# Disk + Spherical Halo

## A NUMERICAL STUDY OF THE STABILITY OF FLATTENED GALAXIES: OR, CAN COLD GALAXIES SURVIVE?\*

J. P. Ostriker

Princeton University Observatory

AND

P. J. E. Peebles

Joseph Henry Laboratories, Princeton University

*Received 1973 May 29*

### ABSTRACT

To study the stability of flattened galaxies, we have followed the evolution of simulated galaxies containing 150 to 500 mass points. Models which begin with characteristics similar to the disk of our Galaxy (except for increased velocity dispersion and thickness to assure local stability) were found to be rapidly and grossly unstable to barlike modes. These modes cause an increase in random kinetic energy, with approximate stability being reached when the ratio of kinetic energy of rotation to total gravitational energy, designated  $t$ , is reduced to the value of  $0.14 \pm 0.02$ . Parameter studies indicate that the result probably is not due to inadequacies of the numerical  $N$ -body simulation method. A survey of the literature shows that a critical value for limiting stability  $t \simeq 0.14$  has been found by a variety of methods.

Models with added spherical (halo) component are more stable. It appears that halo-to-disk mass ratios of 1 to  $2\frac{1}{2}$ , and an initial value of  $t \simeq 0.14 \pm 0.03$ , are required for stability. If our Galaxy (and other spirals) do not have a substantial unobserved mass in a hot disk component, then apparently the halo (spherical) mass interior to the disk must be comparable to the disk mass. Thus normalized, the halo masses of our Galaxy and of other spiral galaxies exterior to the observed disks may be extremely large.

# Disk Instability

## The stability and masses of disc galaxies

G. Efstathiou<sup>1,2</sup>, G. Lake<sup>1,2,3</sup> and J. Negroponte<sup>4</sup>

<sup>1</sup>*Institute of Astronomy, Madingley Road, Cambridge CB3 0HA*

<sup>2</sup>*Department of Astronomy and Space Sciences Laboratory, University of California, Berkeley, California 94720, USA*

<sup>3</sup>*Bell Laboratories, Murray Hill, NJ 07974, USA*

<sup>4</sup>*Department of Physics, University of California, Berkeley, California 94720, USA*

Received 1981 November 12; in original form 1981 September 2

**Summary.** Using  $N$ -body experiments we investigate the global stability of a series of models designed to match the observed photometric and kinematic properties of disc galaxies. The models, therefore, have an exponential surface density profile and rotation curves which are flat at large radii. We find a simple delineator of stability to bar-like modes for a cold disc:  $v_m / (\alpha M_D G)^{1/2} = 1.1$ , where  $v_m$  is the maximum rotational velocity,  $\alpha^{-1}$  is the scale length of the exponential disc and  $M_D$  is the total disc mass. This is to be compared to a self-gravitating exponential disc for which  $v_m / (\alpha M_D G)^{1/2} = 0.63$ , thus a hot 'halo' component is required to increase this ratio in a cool disc and provide stability to bar formation. This criterion has been found to apply independent

Total: Disk+Halo

$$\epsilon_m \equiv \frac{V_{\max}}{(GM_d/R_d)^{1/2}}$$

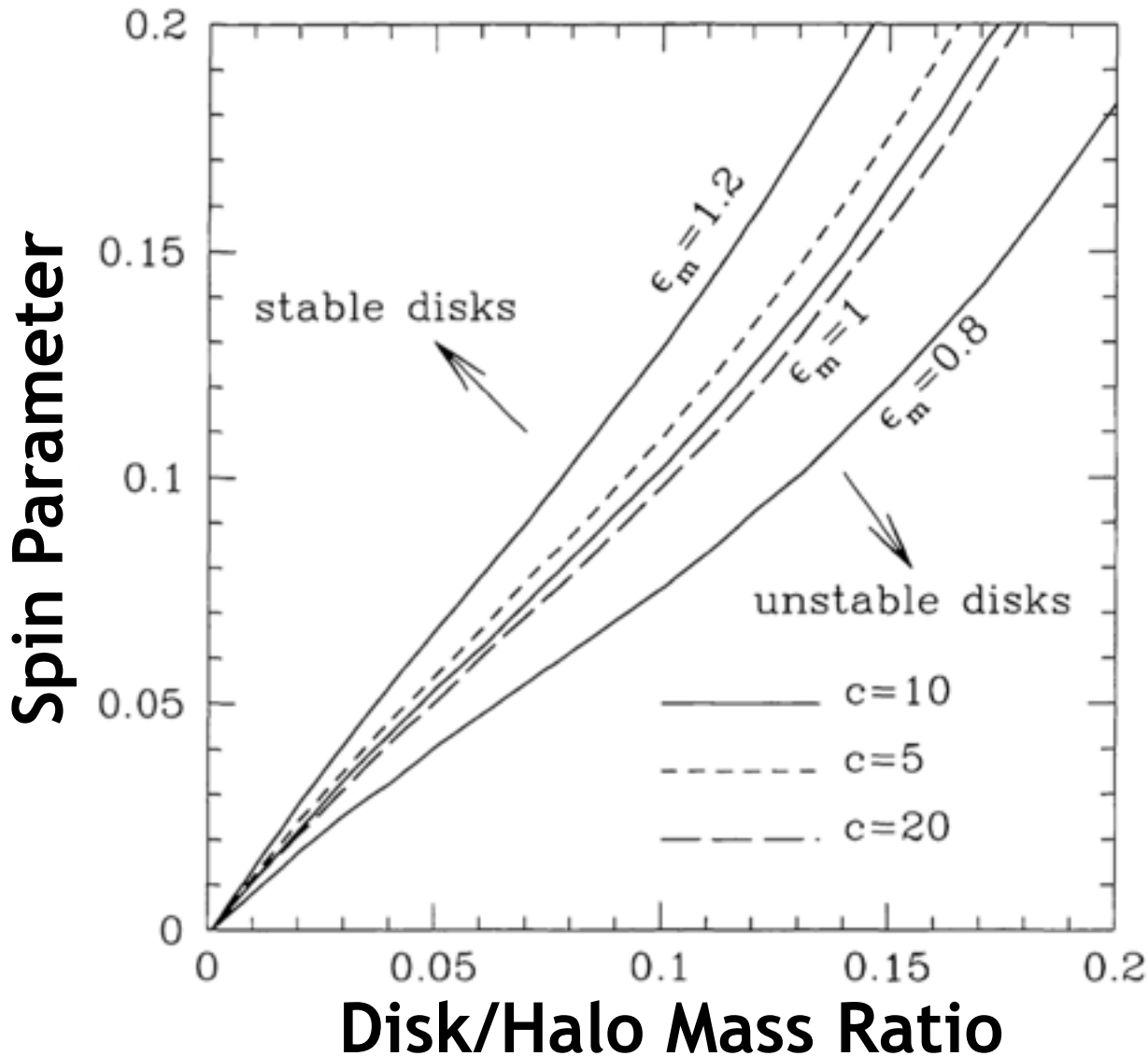
Disk

Stable disk  $\epsilon_m > 1.1$

Unstable disk  $\epsilon_m < 1.1$

Isolated disk  $\epsilon_m \equiv 0.63$

# Semi-Analytical Models



$$\epsilon_m \equiv \frac{V_{\max}}{(GM_d/R_d)^{1/2}} \lesssim 1.1,$$

Efstathiou et al 1982

$$f_{disc} = \frac{V_c(r_{50})}{\sqrt{GM_{disc}/r_{50}}},$$

Cole et al 2000

Bower et al 2006

Mo Mao & White 1998



# Cosmological Simulations

Previous work based exclusively in zoom-in technique:

**Curir et al. 2006; Scannapieco & Athanassoula 2012 and Okamoto et al 2014** using the Aquarius simulations of individual Milky Way halos study the formation of two barred galaxies in the  $\Lambda$ CDM cosmological model. They show that barred galaxies can form naturally in this model.

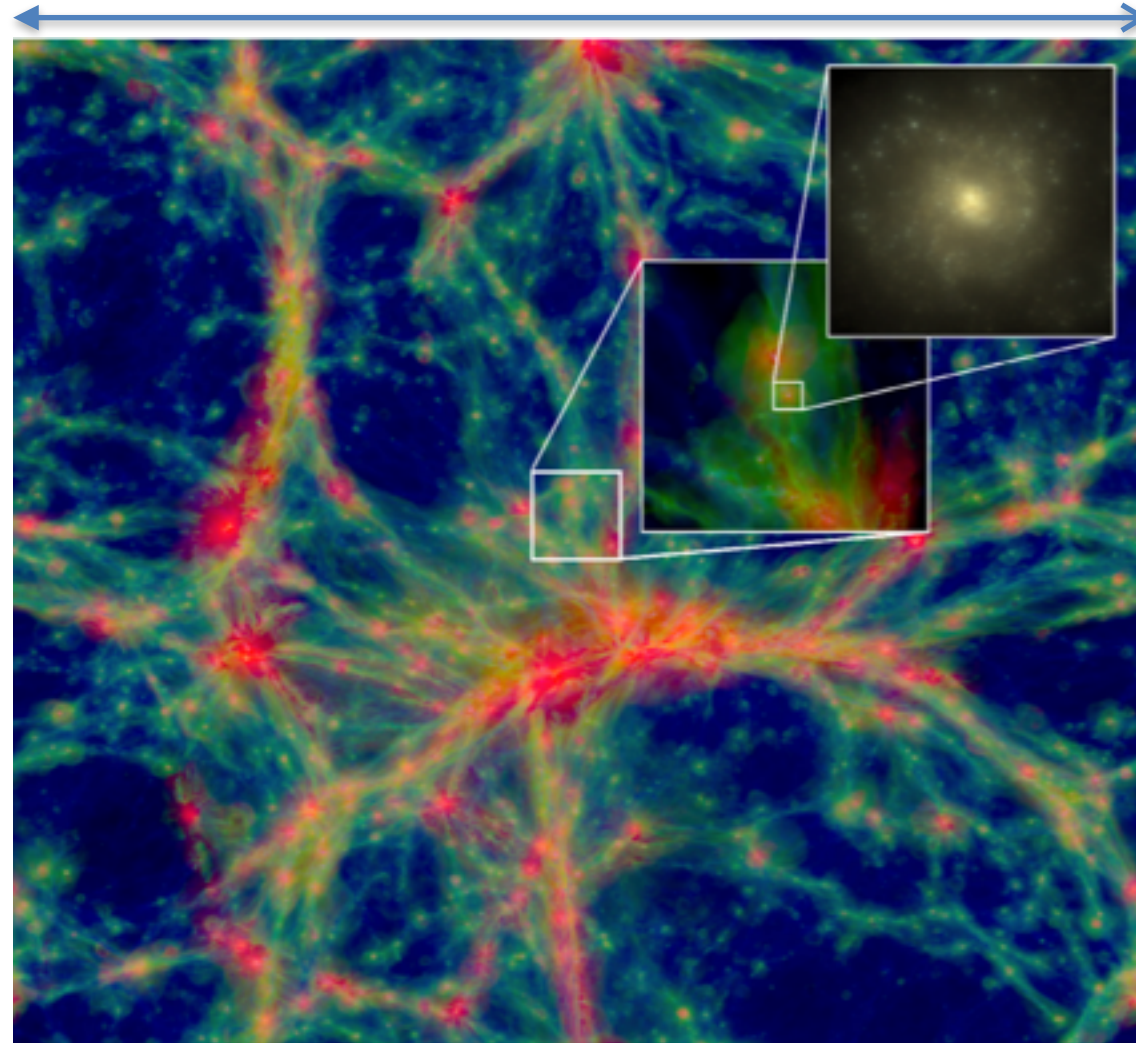
**Kraljic et al. (2012)** using RAMSES study the evolution of bars in a sample of 33 zoom-in simulated galaxies. **Guedes et al. 2013; Goz et al (2015)** two barred galaxies with two different resolution.

Aim:

Extend disk work to a more statistically significant sample.

# EAGLE Cosmological Simulations

100 Mpc (Gas)



60 kpc (Stars)  
 $M=3 \times 10^{10} M_{\odot}$

## Physical Process:

Gravity, Hydrodynamics, Radiative gas cooling, Star formation, Feedback from Supernovae + AGN  
Metallicity

## Particles:

Gas, stars and dark matter.  
 $M_{\text{gas}}=1.81 \times 10^6 M_{\odot}$   
 $M_{\text{dark}}=9.70 \times 10^6 M_{\odot}$

## Code:

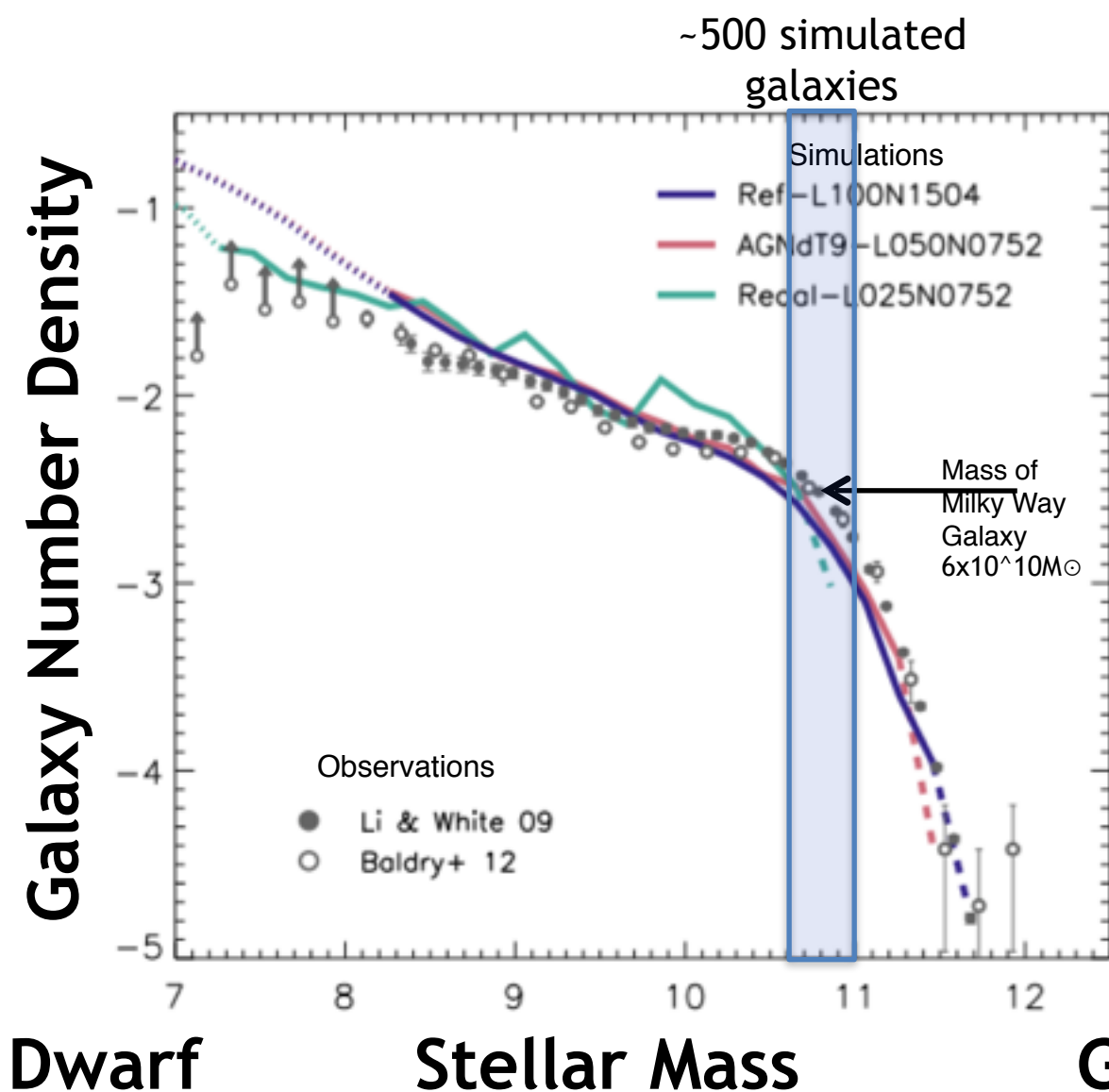
GADGET-3 Springel et al 2005

## Cosmological Parameters:

$\Lambda$ CDM model Planck et al 2014

Schaye et al 2015

# Stellar Mass Function



The galaxy stellar mass function at  $z = 0.1$  for the EAGLE simulations compared to observations.

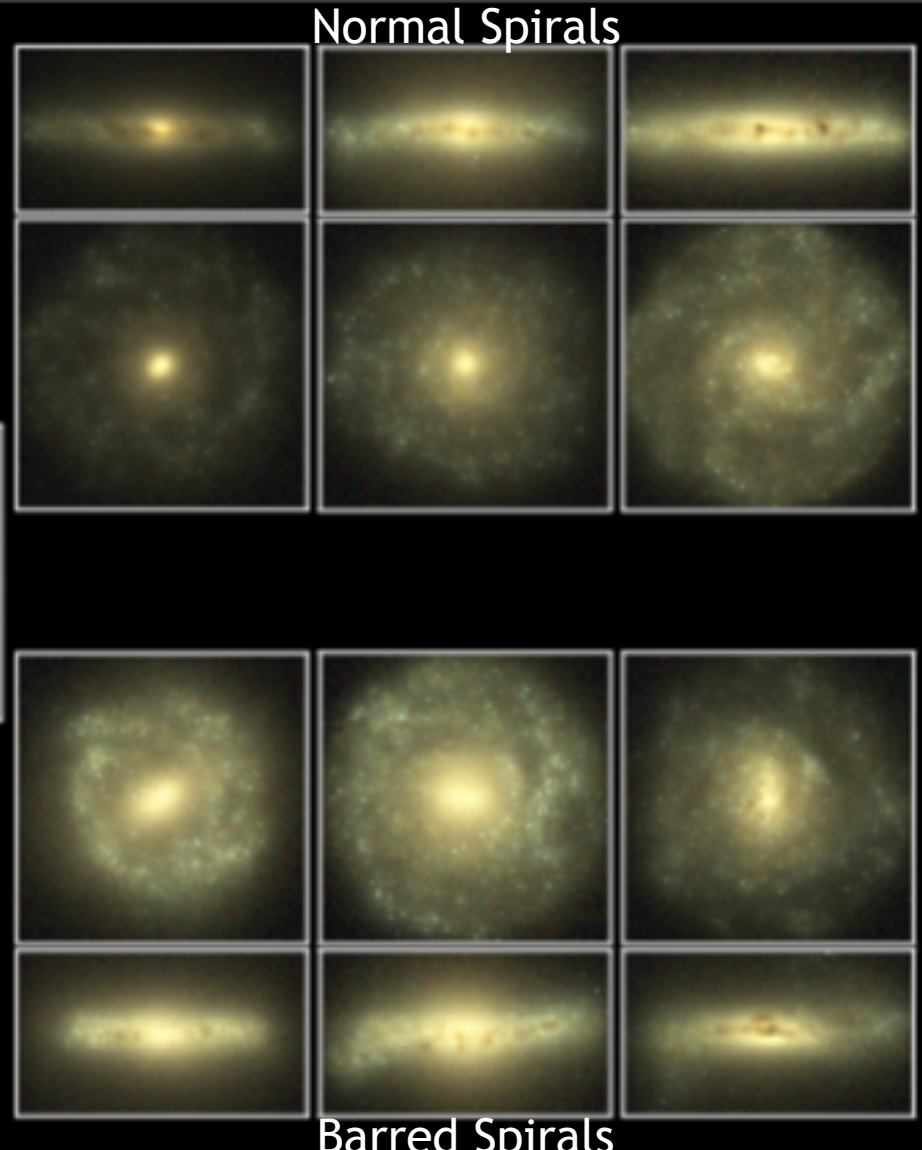
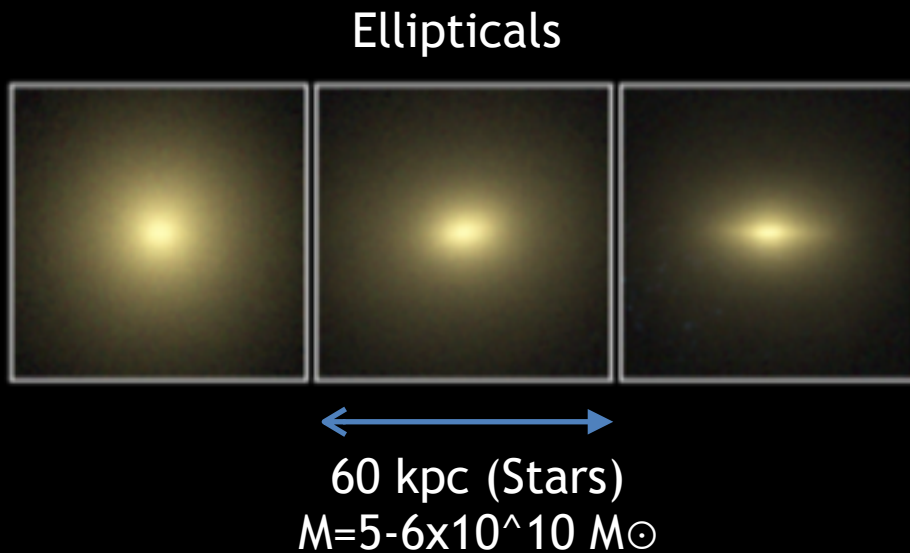
The galaxy number density agrees with the data to  $< \sim 0.2$  dex.

High-mass end fewer than 10 objects per (0.2 dex) stellar mass bin.

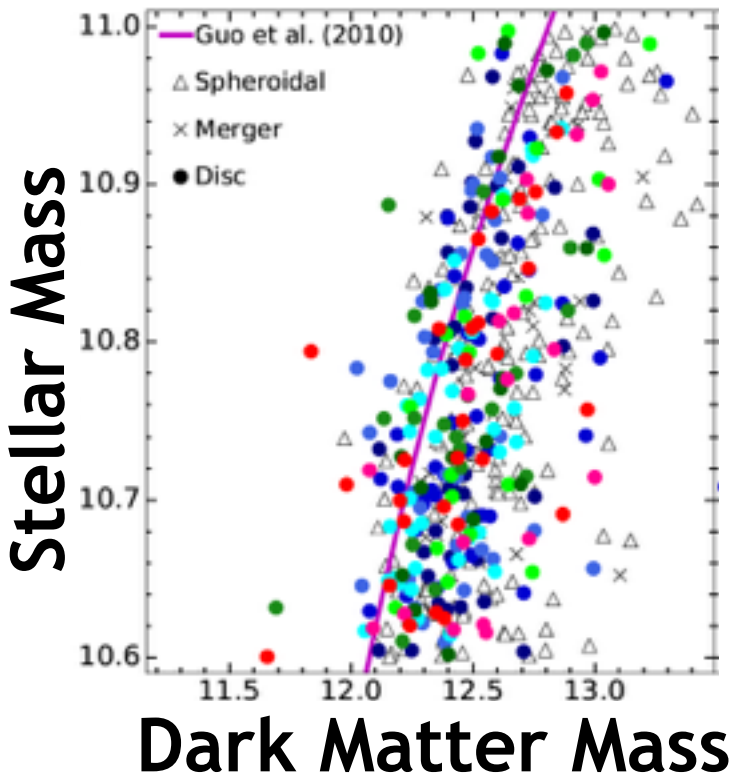
Low-mass end stellar mass falls below 100 baryonic particles.

GAMA survey ( $z < 0.06$ ; Baldry et al. 2012) SDSS ( $z \sim 0.07$ ; Li & White 2009).

# EAGLE Morphological Classification

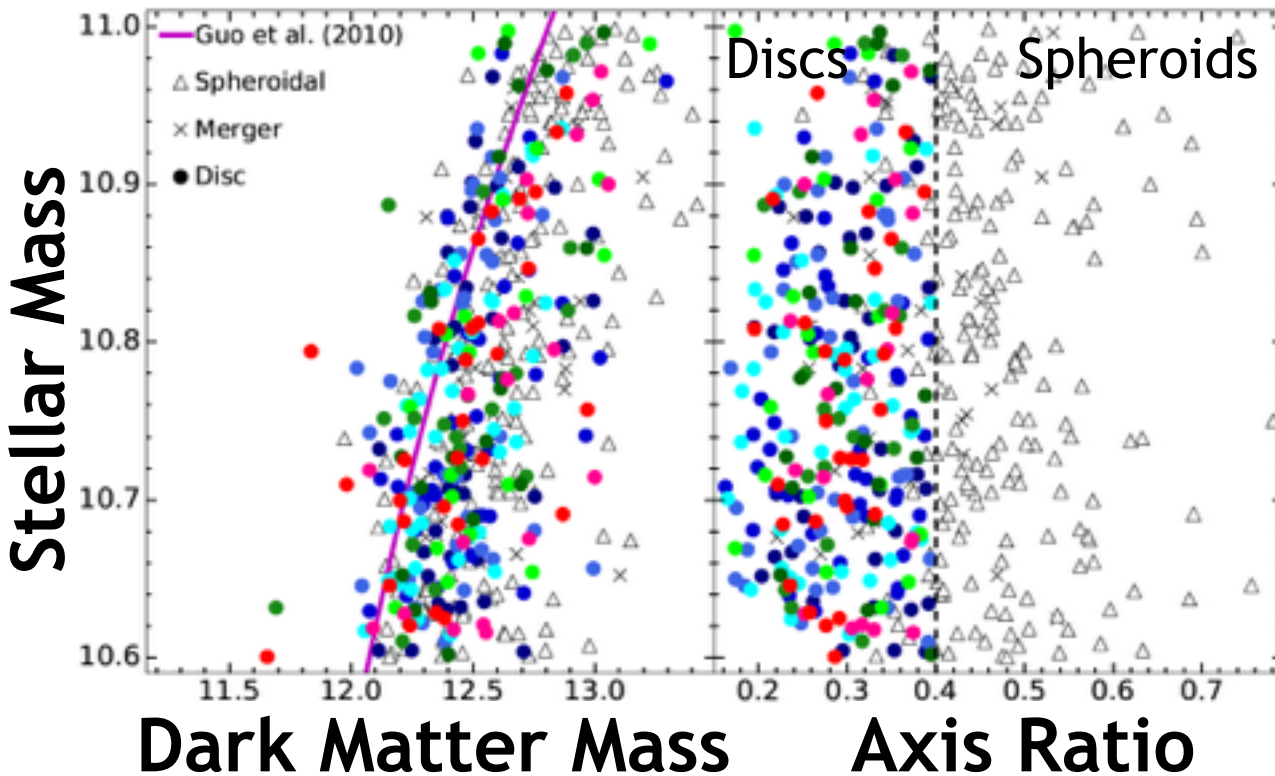


# Disk Galaxy Sample Selection



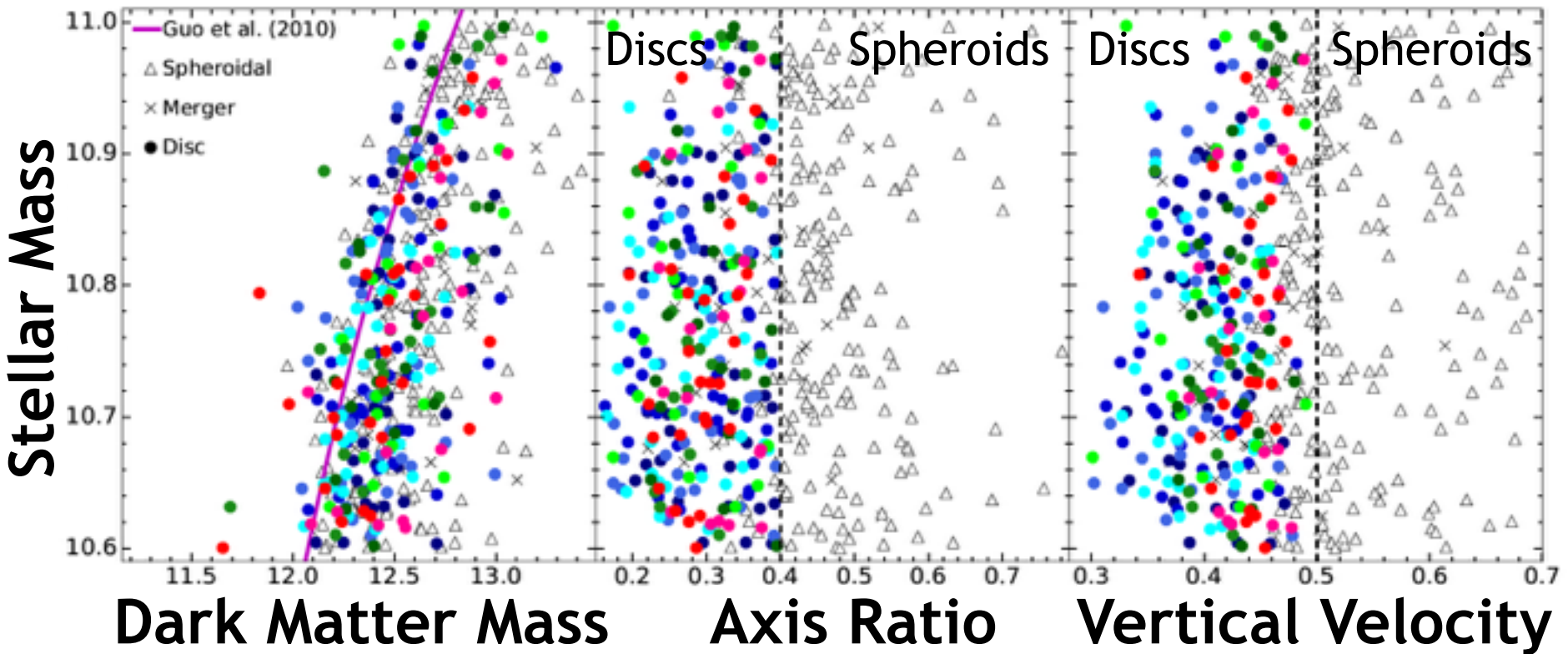
Disc galaxy sample from EAGLE used in this paper. Left: Galaxy stellar mass,  $M$ , as a function virial mass  $M_{200}$ . Solid line indicates the prediction of the abundance-matching model of [Guo et al. \(2010\)](#), for reference. Middle: Flattening parameter  $c=a$ , measured as the ratio of the eigenvalues of the principal axes of the inertia tensor of the stars. Right: Minor axis stellar velocity dispersion, expressed in units of the total. Vertical dashed lines indicate the conditions required to be selected as “discs” in our analysis. Discs are shown as coloured circles, spheroidal systems as open triangles, and visually identified ongoing mergers or disturbed systems as crosses. The colour scheme denotes the strength of the bar pattern.

# Disk Galaxy Sample Selection



Disc galaxy sample from EAGLE used in this paper. Left: Galaxy stellar mass,  $M$ , as a function virial mass  $M_{200}$ . Solid line indicates the prediction of the abundance-matching model of [Guo et al. \(2010\)](#), for reference. Middle: Flattening parameter  $c=a$ , measured as the ratio of the eigenvalues of the principal axes of the inertia tensor of the stars. Right: Minor axis stellar velocity dispersion, expressed in units of the total. Vertical dashed lines indicate the conditions required to be selected as “discs” in our analysis. Discs are shown as coloured circles, spheroidal systems as open triangles, and visually identified ongoing mergers or disturbed systems as crosses. The colour scheme denotes the strength of the bar pattern.

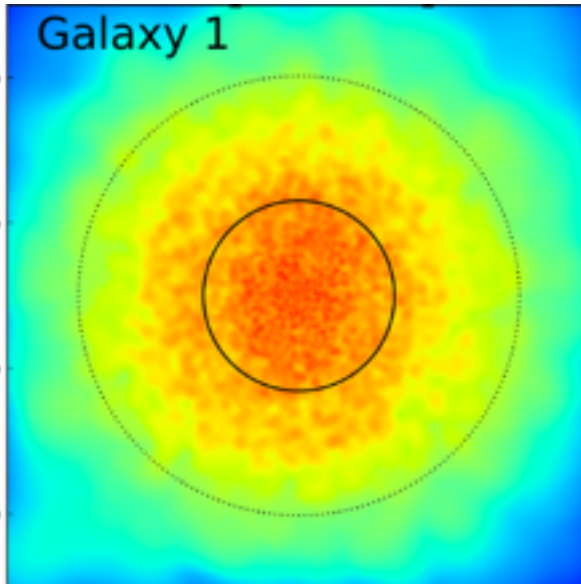
# Disk Galaxy Sample Selection



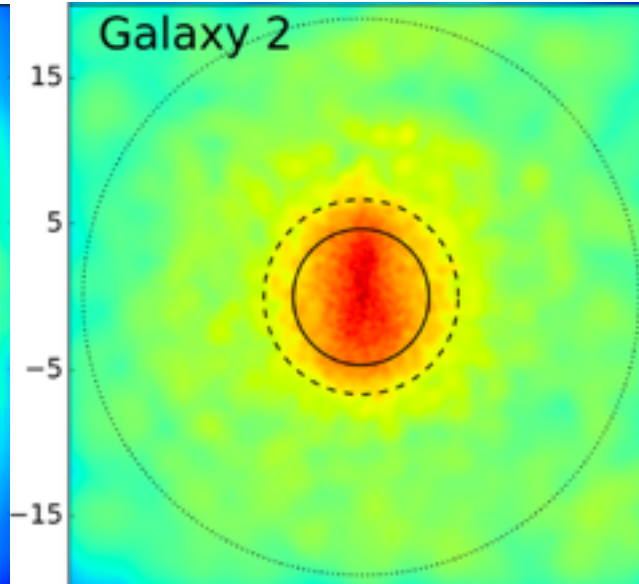
Disc galaxy sample from EAGLE used in this paper. Left: Galaxy stellar mass,  $M$ , as a function virial mass  $M_{200}$ . Solid line indicates the prediction of the abundance-matching model of Guo et al. (2010), for reference. Middle: Flattening parameter  $c=a$ , measured as the ratio of the eigenvalues of the principal axes of the inertia tensor of the stars. Right: Minor axis stellar velocity dispersion, expressed in units of the total. Vertical dashed lines indicate the conditions required to be selected as “discs” in our analysis. Discs are shown as coloured circles, spheroidal systems as open triangles, and visually identified ongoing mergers or disturbed systems as crosses. The colour scheme denotes the strength of the bar pattern.

# Face-On Galaxies

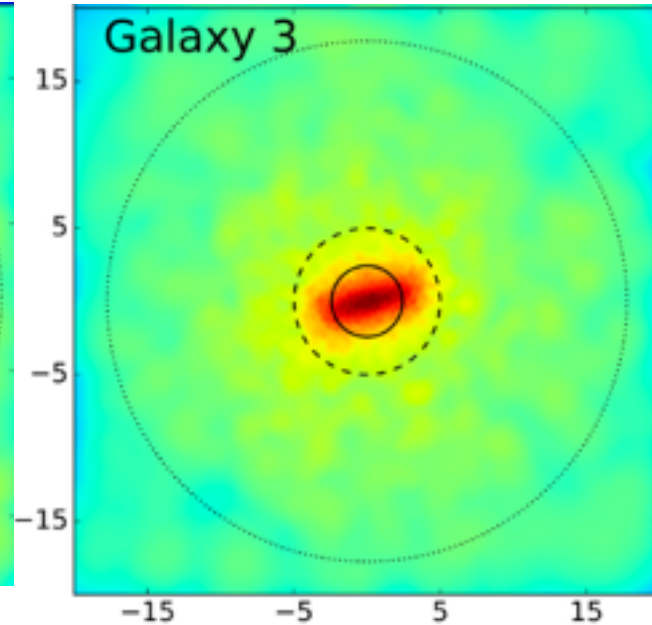
Unbarred



Weak Bar



Strong Bar



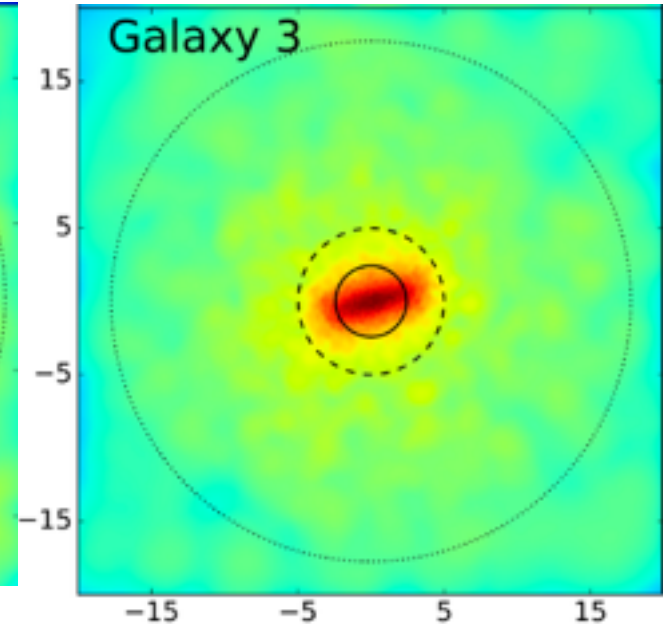
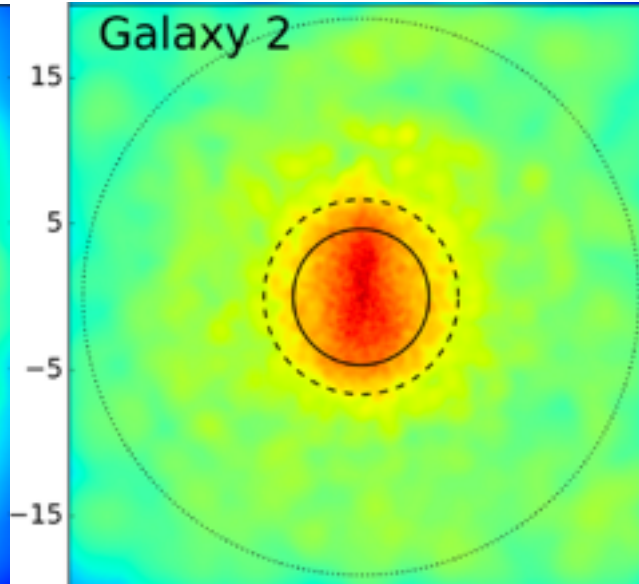
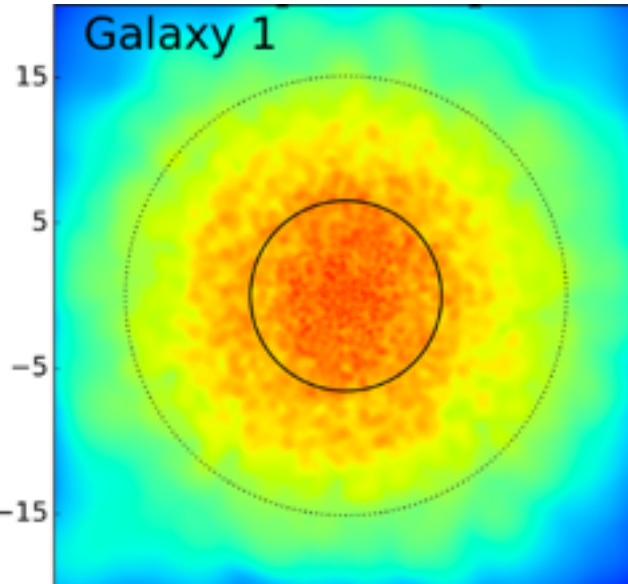



# Bar Strength Parameter


Unbarred

Weak Bar

Strong Bar



  
A2=0

  
A2=1

$$a_m(R) = \sum_{i=1}^{N_R} m_i \cos(m\theta_i)$$

$$b_m(R) = \sum_{i=1}^{N_R} m_i \sin(m\theta_i)$$

$$I_m(R) = \sqrt{a_m^2 + b_m^2}$$

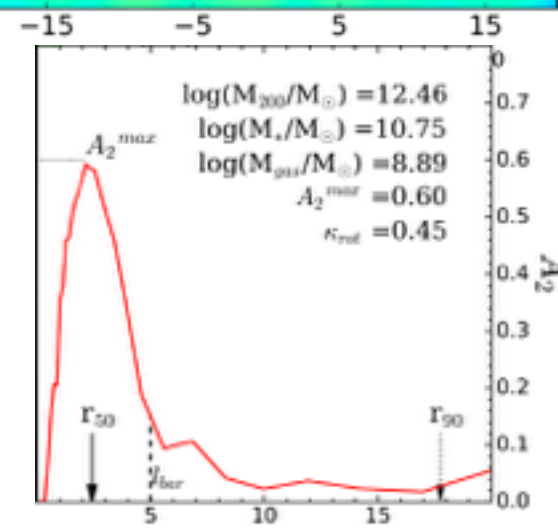
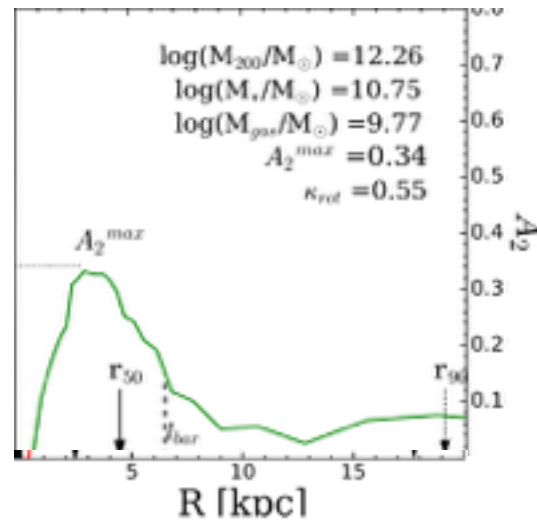
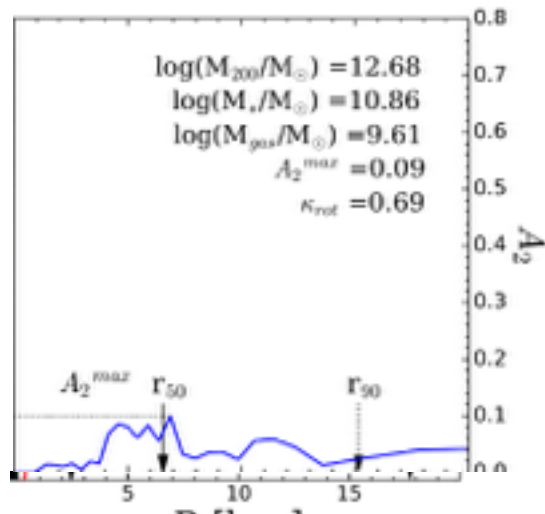
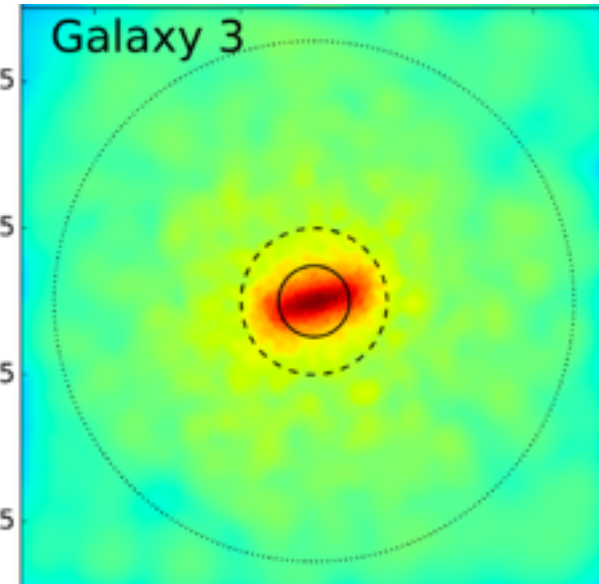
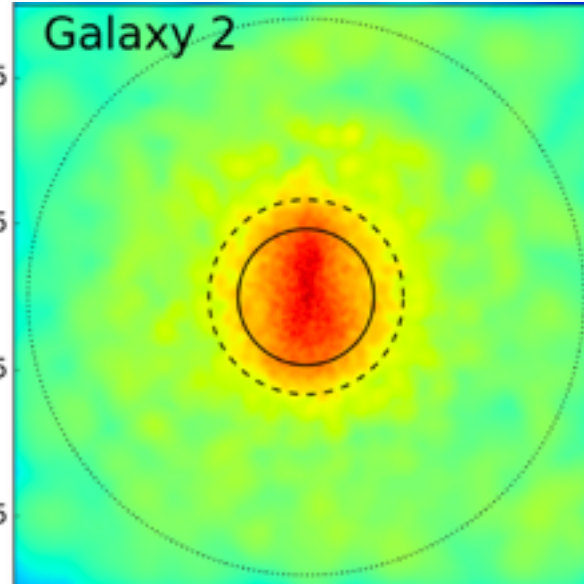
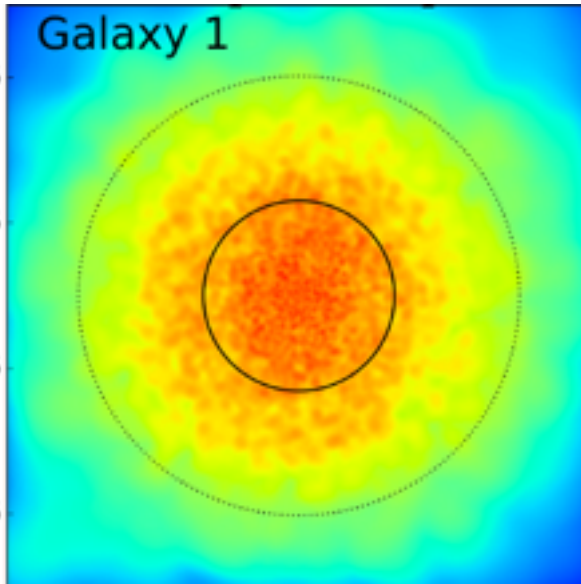
$$A_2(R) = \frac{I_2}{a_0}$$

# Bar Strength Radial Profile

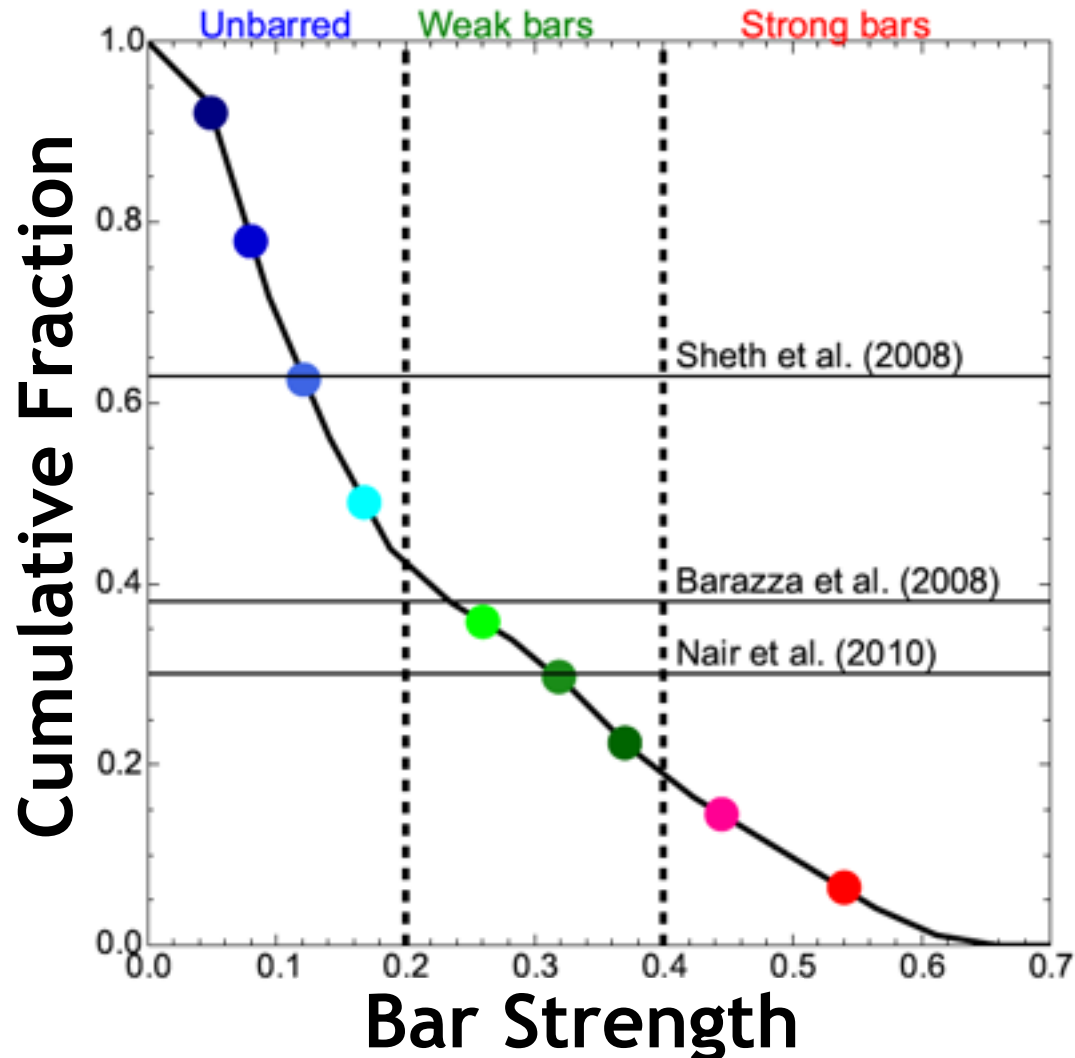
Unbarred

Weak Bar

Strong Bar



# Abundance of Barred Galaxies



Cumulative galaxy fraction as function of bar strength parameter  $A2\_max$  in the local Universe.

About 40% of EAGLE discs have bars (weak or strong) seems quite consistent with observations: Barazza et al. (2008)  $\sim 38\%$ , Sheth et al. (2008)  $\sim 62\%$   
Nair & Abraham (2010)  $\sim 30\%$ .

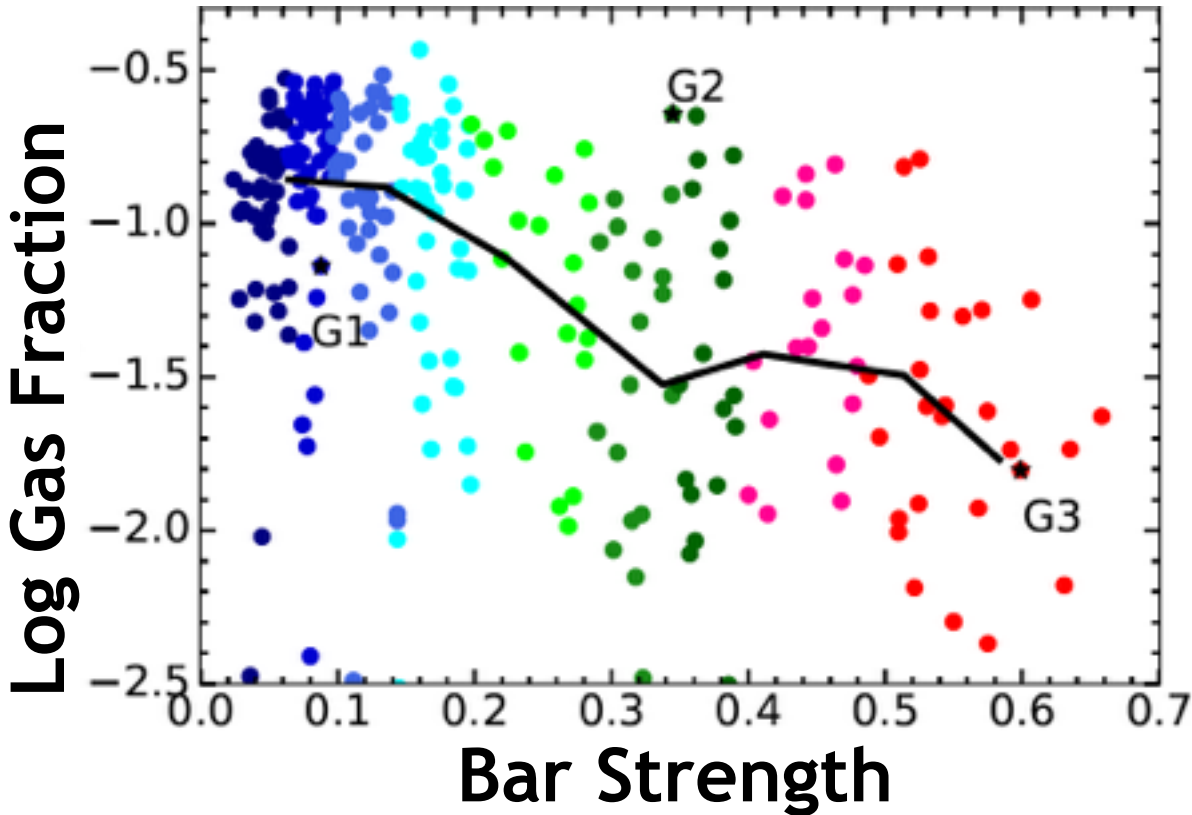
No standard definition of a bar. Bar prominence depends on the photometric band (stronger in the infrared), morphological type (longer in early-type spirals), galaxy mass (decreasing with increasing mass) and redshift (less frequent at early times).

# Gas Mass vs Bar Strength

Unbarred

Weak Barred

Strong Barred



Bars are relatively gas poor

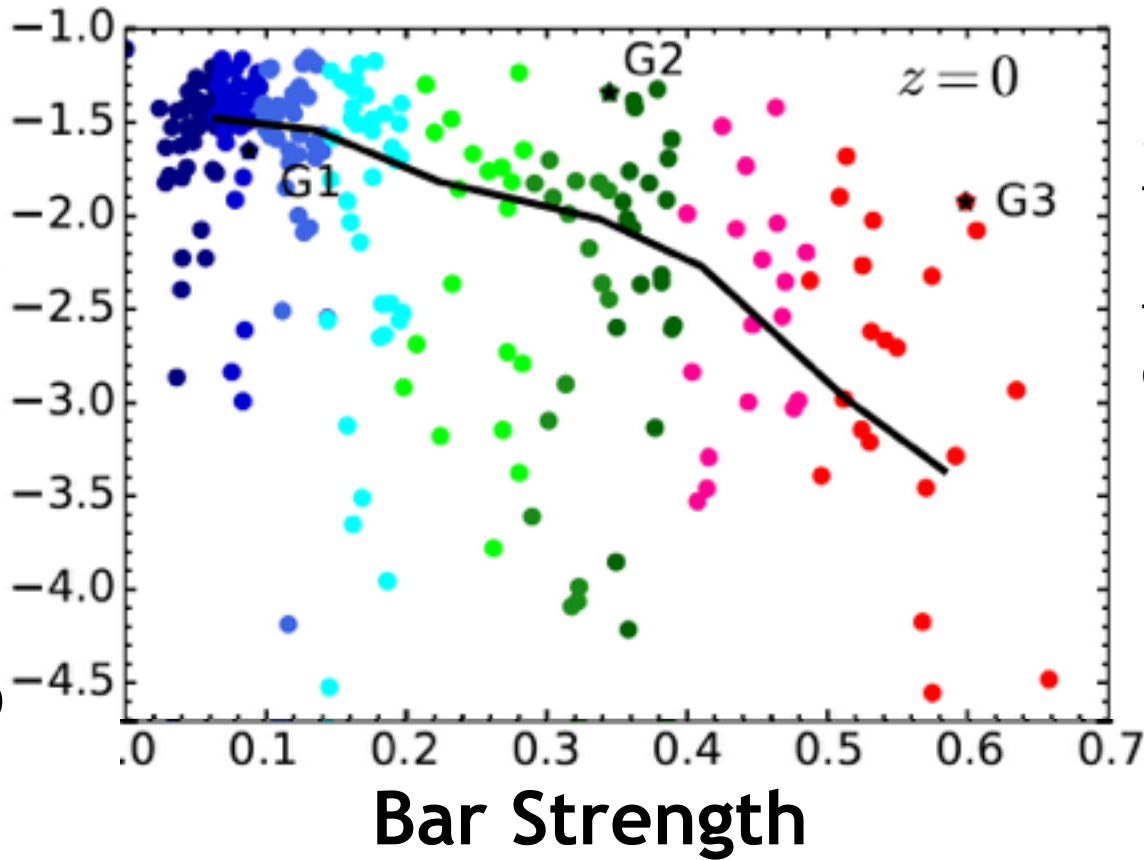
# Star Formation vs Bar Strength

Log Star Formation Rate

Unbarred

Weak Barred

Strong Barred



Bars are relatively gas poor

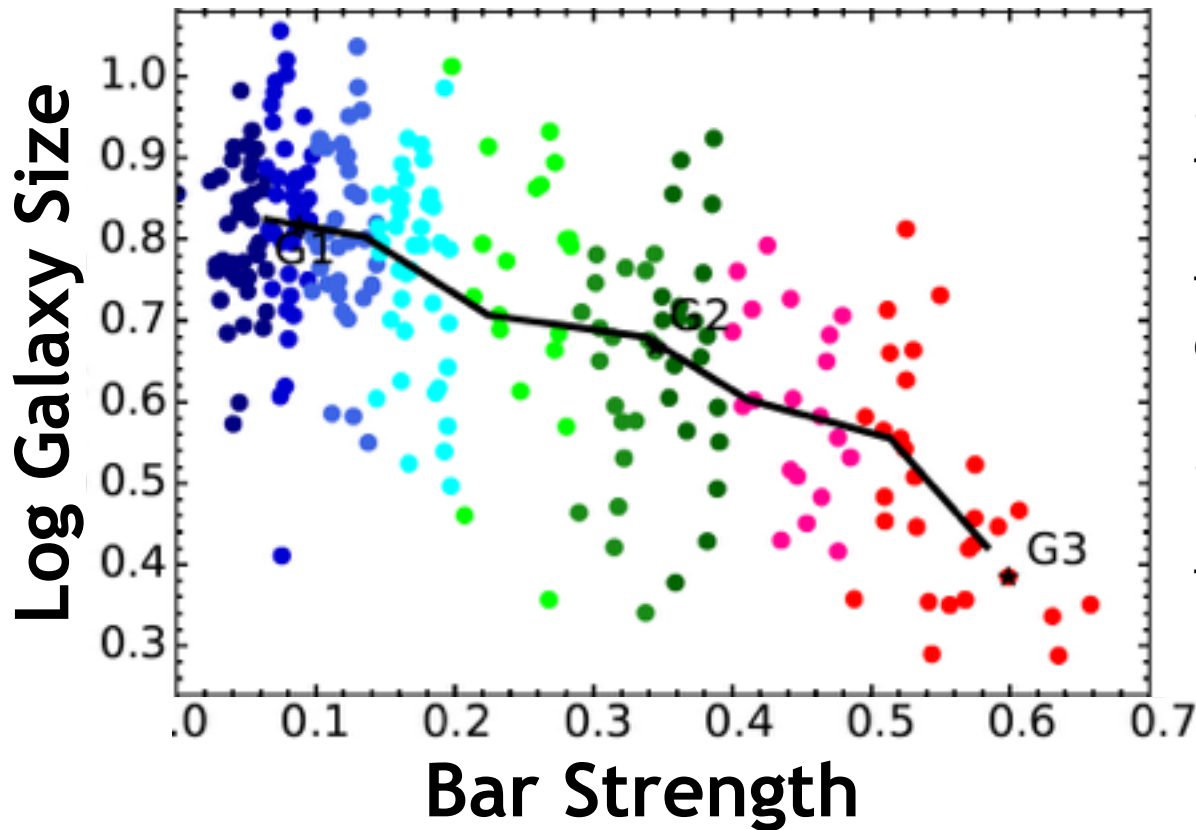
Star formation rates  $\sim 40\%$  of their past average for unbarred galaxies, decreasing to 1% for strongly barred ones.

# Size vs Bar Strength

Unbarred

Weak Barred

Strong Barred

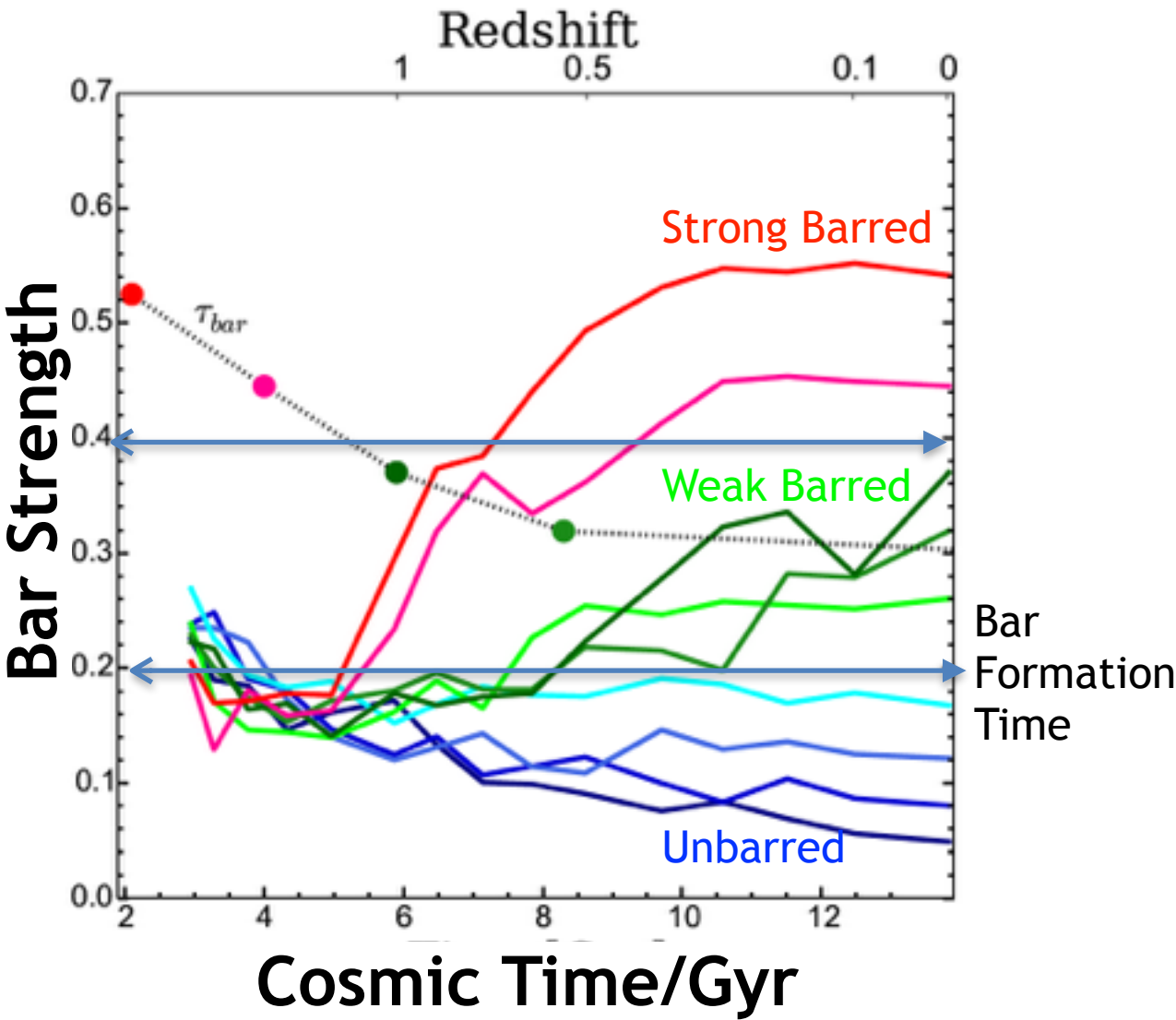


Bars are relatively gas poor

Star formation rates  $\sim 40\%$  of their past average for unbarred galaxies, decreasing to 1% for strongly barred ones.

Strongly-barred discs are roughly three times smaller than unbarred systems

# Bar Growth



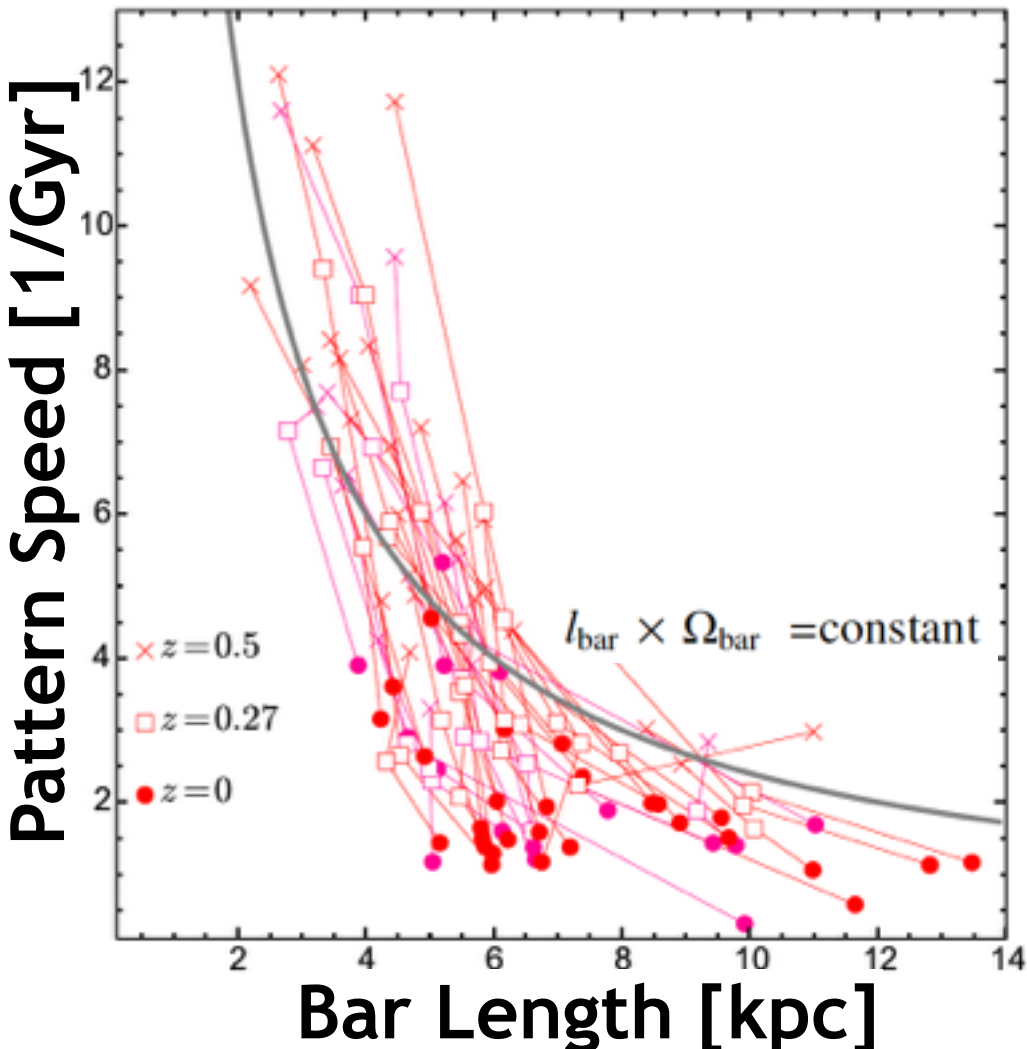
Strong bars develop quickly and saturate

Weak bars are still growing at  $z = 0$ .

Few unbarred galaxies have had bars in the past.

Timescale for bar growth is clearly a strong function of final bar strength.

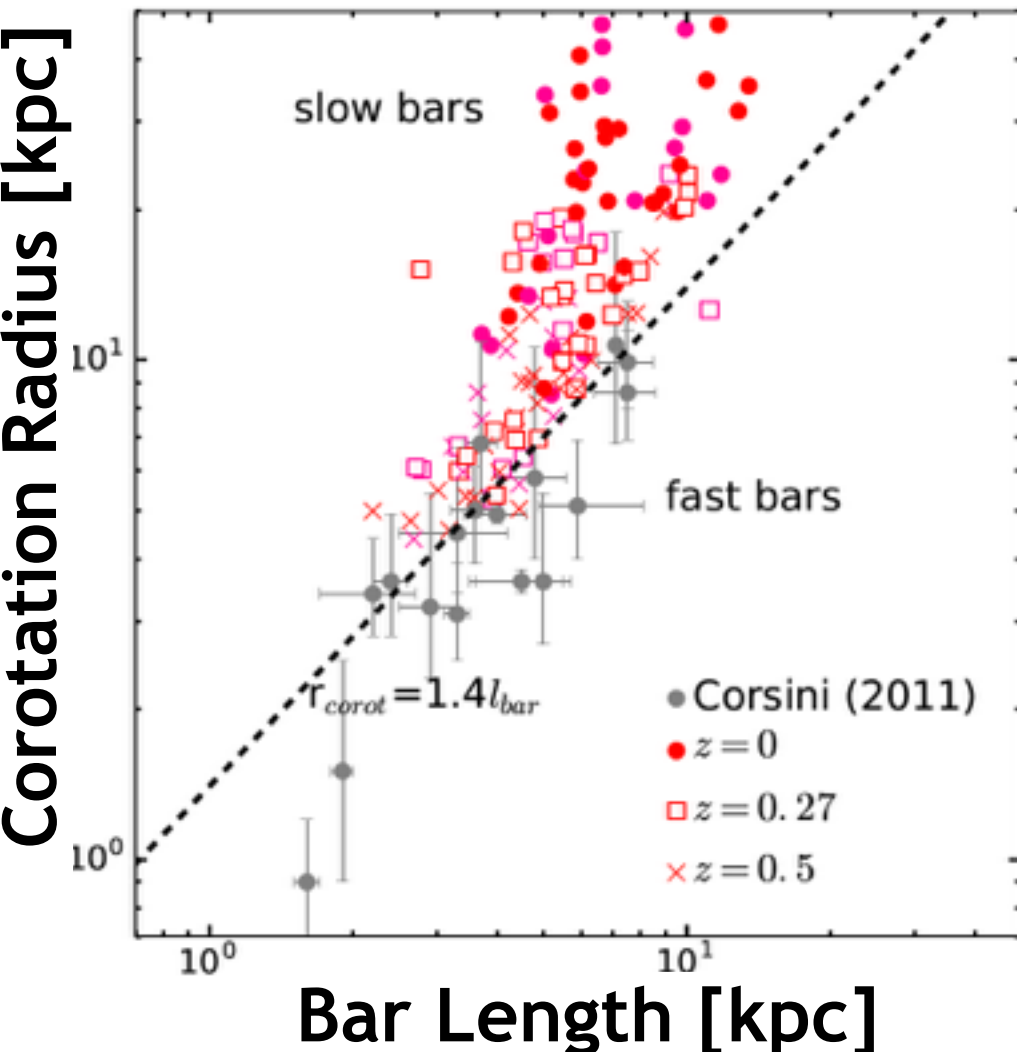
# Bar Growth and Slowdown



Bars slow down  
as they grow.



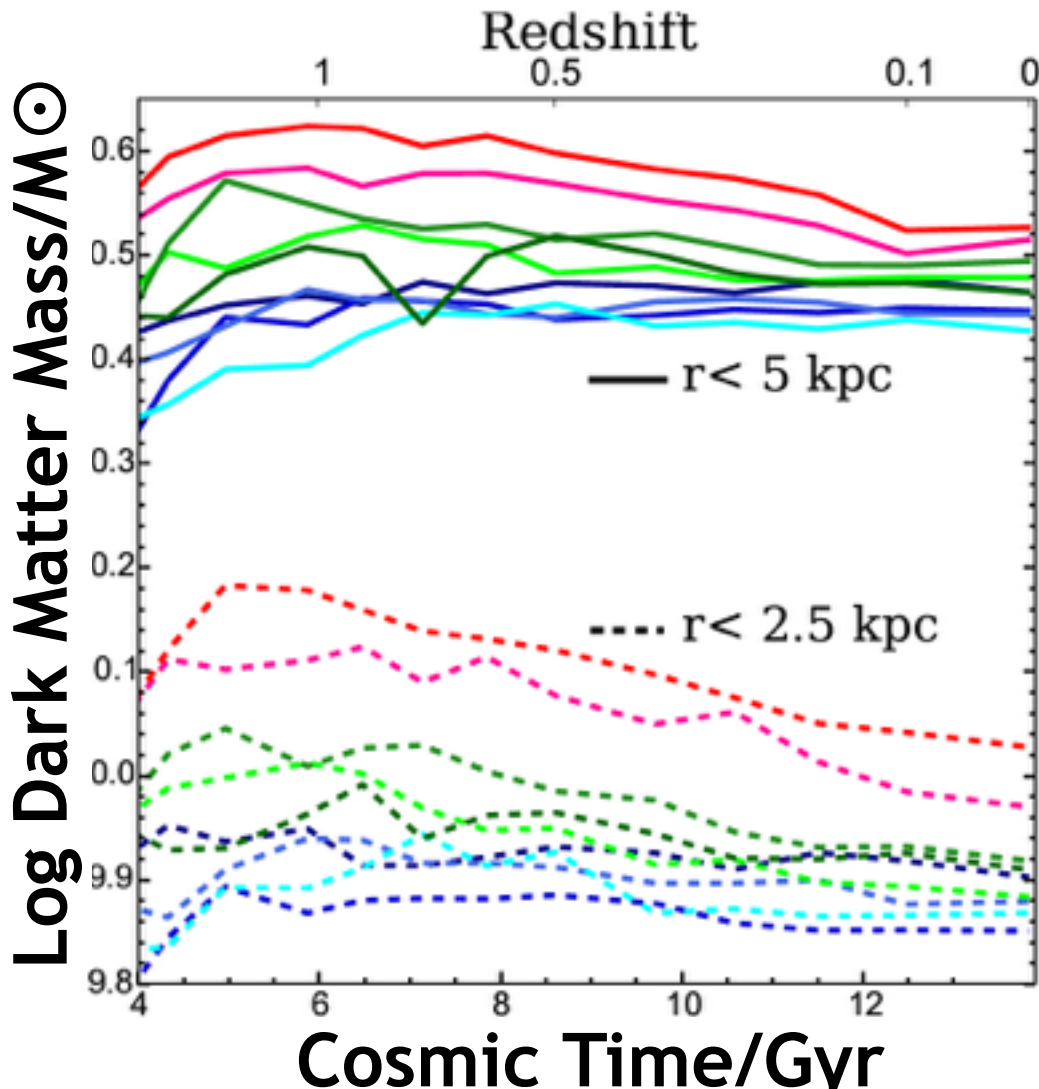
# Bar Slowdown



$z = 0.5$  (triangles),  $z = 0.27$  (squares), and  $z = 0$  (circles). Grey symbols with error bars are observational data from the compilation of Corsini (2011).

“Fast bars” are those below the dotted line delineating  $r_{corot} = 1:4 l_{bar}$ . Most strong bars in our simulation are “slow” at  $z = 0$ , in contrast with observational estimates.

# Dark Matter Halo Evolution



Bar slowdown clearly reduces the central density of dark matter within the region of the bar.

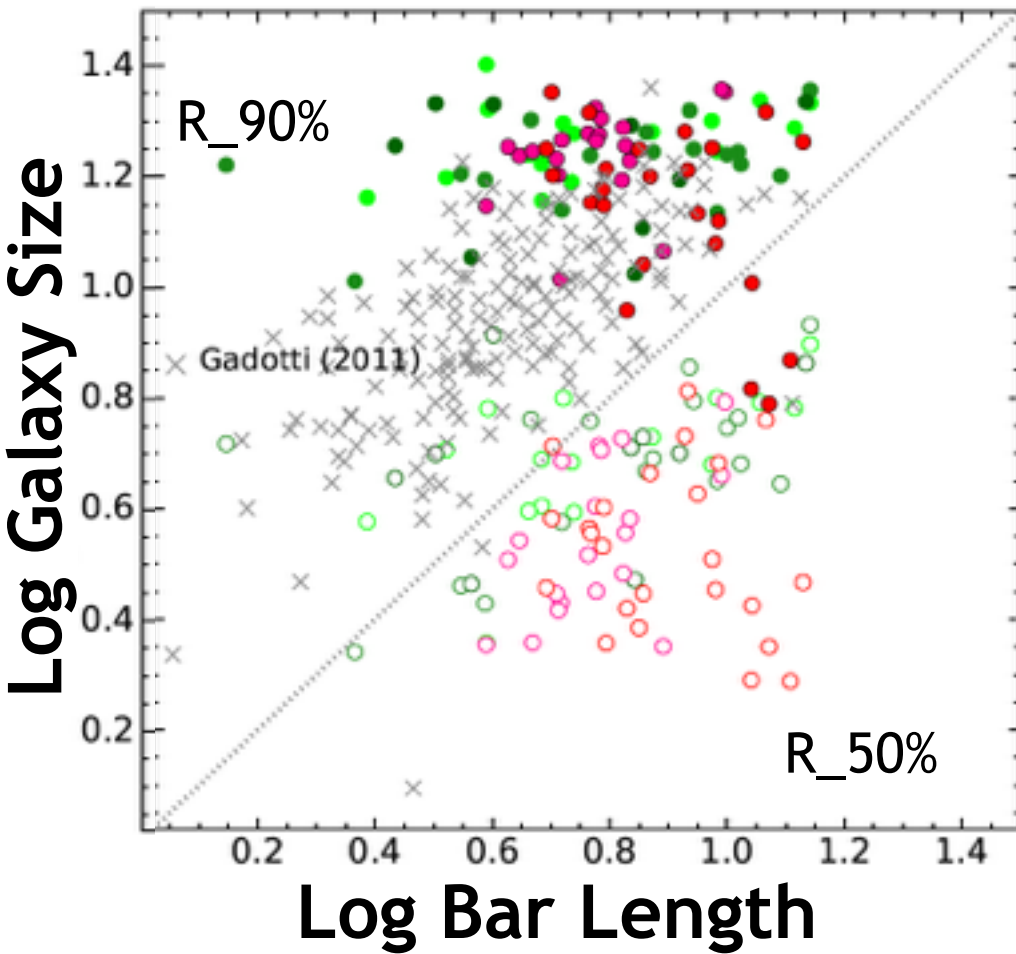
By contrast, the central dark matter densities of unbarred galaxies remain unchanged during the past 5-6 Gyr.

# Conclusions

- 1) 20% strong bars, 20% weak bars, 60% unbarred. This bar frequency seems in reasonable agreement with observational estimates
- 2) Bars develop preferentially in systems where the disc is gravitationally important
- 3) Stronger bars develop in systems that are less gas-rich, and that have formed the bulk of their stars earlier than unbarred discs.
- 4) Strong bars develop relatively quickly before saturating but weak bars are still growing in strength
- 5) Strong bars slow down quickly as they grow
- 6) Bar slowdown induces an expansion of the inner regions of the dark matter halo

# Bar Length

Weak Barred      Strong Barred

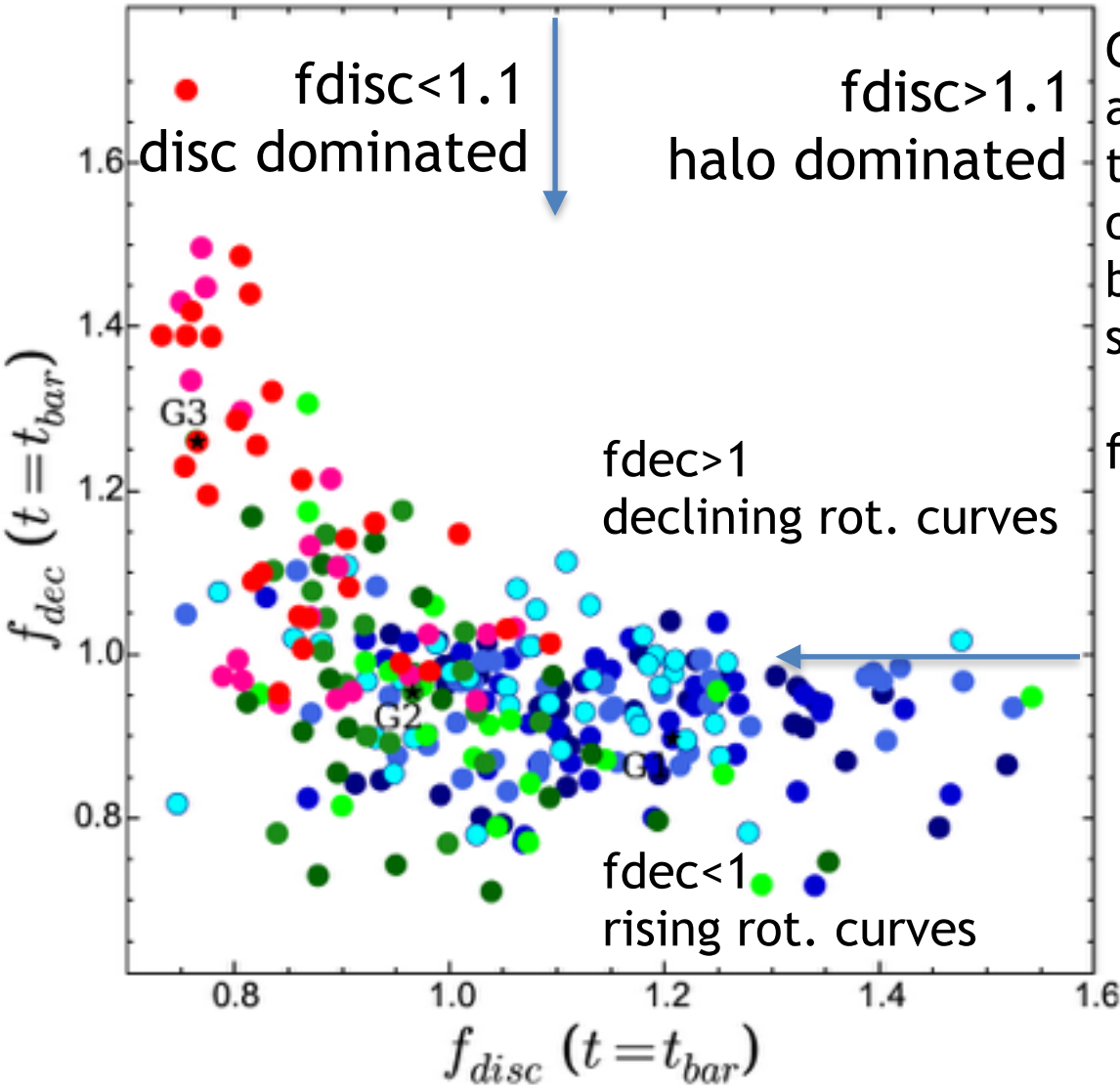


Distribution of bar lengths of nearly 1,000 SDSS (less massive and smaller than our sample) galaxies (Gadotti 2011).

There is no obvious discrepancy between observations and simulations in the regime where they overlap

# Bar Formation Prediction

$$f_{disc} = \frac{V_c(r_{50})}{\sqrt{GM_{disc}/r_{50}}}$$



Galaxies that remain unbarred are predominantly those where the disc is less important, not only within their half-mass radii but also in relation to their surrounding halos.

$$f_{dec} = V_{circ}(R50\%) / V_{max,halo}$$